J|A|C|S
ARTICLES
Published on Web 03/25/2005

Role of Conformation and Electronic Structure in the Chemistry of Ground and Excited State *o*-Pyrazolylphenylnitrenes

Claudio Carra,[†,‡] Thomas Bally,*[,†] and Angelo Albini*[,§]

Contribution from the Department of Chemistry, University of Fribourg, CH-1700 Fribourg, Switzerland, and Department of Chemistry, University of Pavia, I-27100 Pavia, Italy

Received October 2, 2004; E-mail: Thomas.Bally@unifr.ch; Angelo.Albini@unipv.it

Abstract: The chemistry of 2-(1-pyrazolyl)- (**2a**) and 2-[1-(3,5-dimethylpyrazolyl]phenylnitrene (**2b**) has been studied in EtOH solution at room temperature, in EtOH glasses at 90 K, and in Ar matrices at 12 K. These nitrenes were chosen as suitable models for clarifying the mechanism of intramolecular reactions because attack at the pyrazole ring can occur according to different modes and the asymmetry of the substituent gives rise to different conformations. Detailed DFT and CASSCF/CASPT2 studies on the conformation and decay paths of both spin states of the nitrenes have been carried out. Ring expansion to dehydroazepines (via benzoazirines) is calculated to be competitive in both nitrenes, but in the dimethyl derivative, **2b**, attack onto the N lone pair (which is made more nucleophilic by the methyl groups) is favored. The higher barriers (by 4−8 kcal/mol) in singlet **2a** cause 60−70% of this nitrene to decay by intersystem crossing to the triplet. Thus, the seemingly straightforward formation of benzo-fused heterocycles through intramolecular attack of the pyrazoline N lone pair by the singlet phenylnitrene can only overcome ring expansion and intermolecular reactions under favorable circumstances. The comparatively persistent triplet nitrenes are characterized in matrices, and the yields of photocyclization products (mainly pyrazolo[1,5-*a*]benzimidazole (**7**) from **2a** and 5,6-dihydropyrazolo[1,5-*a*]quinoxaline (**8**) from **2b**) are shown to depend on the preferred conformation of the starting azide and nitrene.

1. Introduction

Significant advances in the understanding of the chemistry of arylnitrenes, usually generated by photolysis of aryl azides, and the role of subsequent intermediates have been recently achieved by time-resolved[1−5] and matrix isolation experiments[6−9] supplementing a large body of preceding studies carried out over several decades.[10−17]

Scheme 1

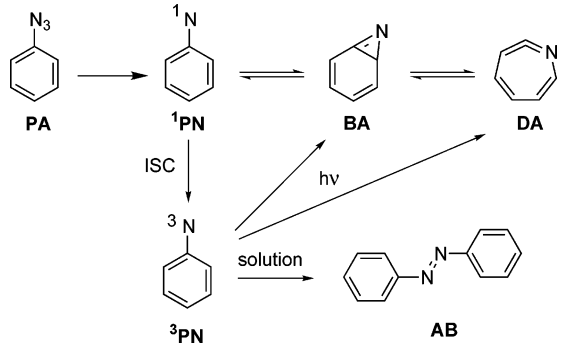

From the synthetic point of view, arylnitrenes have been proven disappointing[16,18] by not undergoing the useful intermolecular insertion and addition reactions of the related arylcarbenes. This is due to rapid rearrangements that prevent intermolecular trapping[16,19] and are usually followed by polymerization, leading to "tars" (see Scheme 1). Thus, isolated yields are often quite low, in particular at azide concentrations

† University of Fribourg.
‡ Present address: Department of Chemistry, University of Ottawa, Canada.
§ University of Pavia.

(1) Gritsan, N. P.; Yuzawa, T.; Platz, M. S. *J. Am. Chem. Soc.* **1997**, *119*, 5059.
(2) Gritsan, N. P.; Zhu, Z.; Hadad, C.; Platz, M. S. *J. Am. Chem. Soc.* **1999**, *121*, 1202.
(3) Gritsan, N. P.; Gudmundsdottir, A. D.; Tigelaar, D.; Zhu, Z.; Karney, W. L.; Hadad, C. M.; Platz, M. S. *J. Am. Chem. Soc.* **2001**, *123*, 1951.
(4) Gritsan, N. P.; Likhotvorik, I.; Tsao, M. L.; Celebi, N.; Platz, M. S.; Karney, W. L.; Kemnitz, C. R.; Borden, W. T. *J. Am. Chem. Soc.* **2001**, *123*, 1425.
(5) Tsao, M. L.; Gritsan, N.; James, T. R.; Platz, M. S.; Hrovat, D. A.; Borden, W. T. *J. Am. Chem. Soc.* **2003**, *125*, 9343.
(6) Chapman, O. L.; LeRoux, J. P. *J. Am. Chem. Soc.* **1978**, *100*, 282.
(7) Hayes, J. C.; Sheridan, R. S. *J. Am. Chem. Soc.* **1990**, *112*, 5879.
(8) Tomioka, H.; Ichikawa, N.; Kamatsu, K. *J. Am. Chem. Soc.* **1993**, *115*, 8621.
(9) Maltsev, A.; Bally, T.; Tsao, M.-L.; Platz, M. S.; Kuhn, A.; Vosswinkel, M.; Wentrup, C. *J. Am. Chem. Soc.* **2003**, *126*, 237.
(10) Smith, P. A. S. In *Azides and Nitrenes: Reactivity and Utility*; Scriven, E. F. V., Ed.; Academic Press: Orlando, FL, 1984; p 95.
(11) Wentrup, C. In *Reactive Intermediates*; Abramovitch, R. A., Ed.; Plenum Press: New York, 1980; Vol. 1; p 263.
(12) Wentrup, C. *Adv. Heterocycl. Chem.* **1981**, *28*, 279.
(13) Wentrup, C. In *Reactive Molecules*; Wiley-Interscience: New York, 1984; Chapter 4.
(14) Platz, M. S.; Leyva, E.; Haider, K. *Org. Photochem.* **1991**, *11*, 367.
(15) Schuster, G. B.; Platz, M. S. *Adv. Photochem.* **1992**, *17*, 69.
(16) Platz, M. S. *Acc. Chem. Res.* **1995**, *28*, 487.
(17) Platz, M. S. In *Reactive Intermediate Chemistry*; Moss, R. A., Platz, M. S., Jones, M., Eds.; Wiley: New York, 2003.
(18) Doering, W. v. E.; Odum, R. A. *Tetrahedron* **1966**, *22*, 81.
(19) Borden, W. T.; Gritsan, N. T.; Hadad, C. M.; Karney, W. L.; Kemnitz, C. R.; Platz, M. S. *Acc. Chem. Res.* **2000**, *33*, 765.

10.1021/ja043988w CCC: $30.25

Scheme 2. Products Obtained after 254-nm Photolysis of Azides 1a and 1b in EtOH under Different Conditions[a]

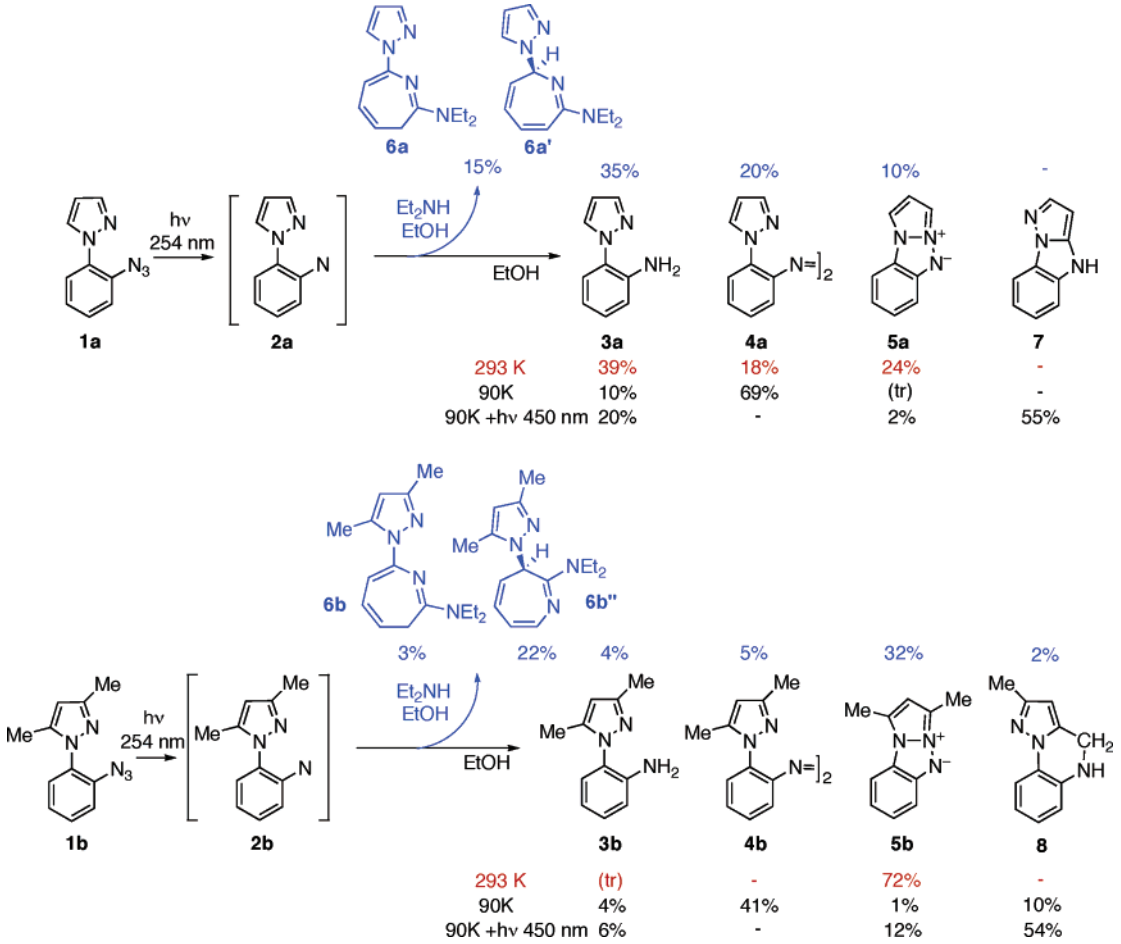

[a] The numbers for **1b** are taken from ref 21. Note that in that paper the values for products **4b** and **8b** were erroneously interchanged.

that are high enough to make reactions preparatively useful. *Intramolecular* trapping reactions are better suited both for obtaining higher yields and for gathering information about the chemistry of nitrenes.[10]

The primary products of phenyl azides (PA) are singlet phenylnitrenes (^{1}PN), which have been identified by flash photolysis[2−5,20] and trapped intermolecularly (in the case of 2,6-difluoro-^{1}PN)[20] or intramolecularly by suitable nucleophiles.[8,21] At room temperature ^{1}PN equilibrates rapidly with the isomeric dehydroazepines (DA) via the metastable benzazirines (BA). These intermediates have also been identified spectroscopically and through trapping by nucleophiles.[18,22,23]

At low temperature (below about 160 K for parent PN and simple derivatives) intersystem crossing (ISC) to the more stable triplet phenylnitrenes (^{3}PN) overwhelms the activated decay processes of the singlet nitrenes and, if diffusion can take place, ^{3}PN dimerize to azobenzenes (AB).[24] In solid matrices, photoexcitation of ^{3}PN yields DA[6,7] (BA in the case of 2,5-difluoro-PN[25]).

An investigation on the photolyis of pyrazolylphenyl azides **1** (Scheme 2)[21,26] contributed to establishing the above picture. The dimethylpyrazolylnitrene **2b** was originally proposed as a mechanistic probe by Suschitzky,[27,28] who expected that intramolecular reactions would allow one to distinguish the electrophilic attack of the N sp^2 lone pair by the singlet vs radical attack of the methyl group by the triplet nitrene. We found that, at room temperature, direct irradiation of **1** does indeed lead to attack of the pyrazole nitrogen by the singlet nitrene, whereas sensitized irradiation leads mainly to azo compounds, which arise by dimerization of triplet nitrenes.[21] In contrast to the usually low yields of products from intermolecular trapping reactions, the material balance was found to be satisfactory (>70%) and thus provided confidence in assessing competing pathways by analysis of product distributions. As with all phenyl azides,[14−17] ISC to ^{3}**2b** became the only process below 160 K, as revealed by UV−vis spectroscopy at 77 K. Upon melting the glass, the triplet nitrene dimerized, with very little hydrogen abstraction from the methyl groups. Photolysis of the 160 K glass resulted in attack at the methyl group, rather than conversion to dehydroazepine DA as with parent ^{3}PN (cf. the discussion in ref 24).

(20) Gritsan, N. P.; Zhai, H. B.; Yuzawa, T.; D, K.; Brooke, J.; Platz, M. S. *J. Phys. Chem. A* **1997**, *101*, 2833.
(21) Albini, A.; Bettinetti, G.; Minoli, G. *J. Am. Chem. Soc.* **1999**, *121*, 3104.
(22) DeGraff, B. A.; Gillespie, D. W.; Sundberg, R. J. *J. Am. Chem. Soc.* **1974**, *96*, 7491.
(23) Carroll, S. E.; Nay, B.; Scriven, E. F. V.; Suschitzky, H.; Thomas, D. R. *Tetrahedron Lett.* **1977**, 3175.
(24) Leyva, E.; Platz, M. S.; Persy, G.; Wirz, J. *J. Am. Chem. Soc.* **1986**, *198*, 3783.
(25) Morawietz, J.; Sander, W. *J. Org. Chem.* **1996**, *61*, 4351.
(26) Albini, A.; Bettinetti, G.; Minoli, G. *J. Am. Chem. Soc.* **1997**, *119*, 7308.
(27) McRobbie, I. M.; Meth-Cohn, O.; Suschitzky, H. *Tetrahedron Lett.* **1976**, 825.
(28) Lindley, J. M.; McRobbie, I. M.; Meth-Cohn, O.; Suschitzky, H. *J. Chem. Soc., Perkin Trans. 1* **1980**, 982.

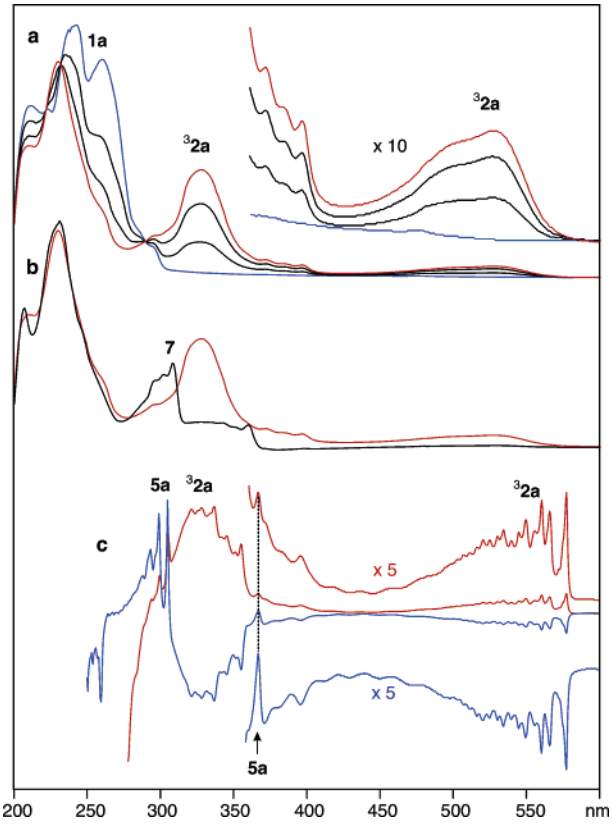

Figure 1. (a) Stepwise 254-nm photolysis of azide **1a** (blue spectrum) in EtOH at 90 K. The visible band of nitrene ^{3}**2a** (red spectrum) is enlarged for better visibility. (b) Photolysis of nitrene ^{3}**2a** (red spectrum) at >450 nm. (c) Difference spectra showing the formation (254 nm photolysis of azide **1a**, red spectrum) and the >515-nm bleaching (blue spectrum) of nitrene ^{3}**2a** in an Ar matrix at 12 K.

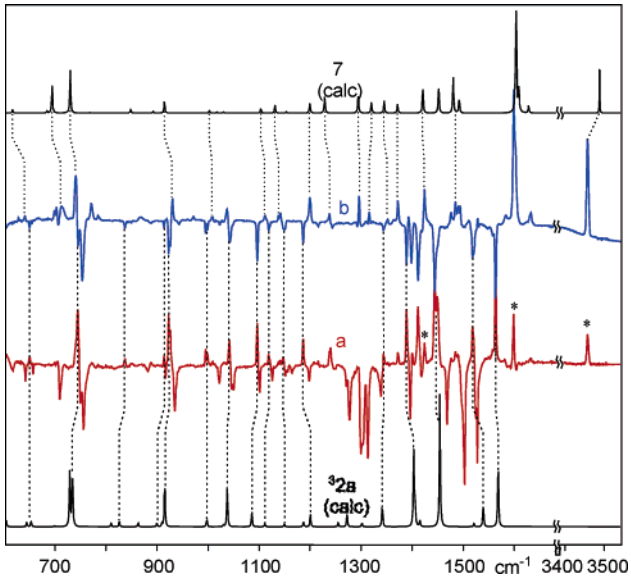

Figure 2. IR difference spectra for (a) the formation (254-nm photolysis of azide **1a**, red spectrum) and (b) the >515-nm bleaching (blue spectrum) of nitrene ^{3}**2a** in an Ar matrix at 12 K. The bands that increase in a and decrease in b (dashed lines) are correlated with those of the simulated spectrum of nitrene ^{3}**2a** at the bottom (B3LYP/6-31G* calculation of most stable conformer). The bands that increase in spectrum b are correlated with those of the simulated spectrum of pyrazoloindole **7** shown at the top (dotted lines).

As **2b** had proven to be a useful model, we decided to extend our previous study to include the parent pyrazolylnitrene, **2a**. This compound lacks the radicalophilic methyl groups but offers the possibility of electrophilic attack on the pyrazole π-system, analogous to the recently reinvestigated case of *o*-biphenylnitrene.[5] **2a** also allowed us to examine whether the conformation of the pyrazole group in the azides or in the incipient nitrenes would affect the reactions, including the competing modes of electrophilic attack. To confront this problem, the intermediates and their chemistry had to be fully characterized in solution and in matrices and the various reaction paths had to be modeled by appropriate methods.

Thus, we investigated the chemistry of nitrene **2a** at room temperature and in an ethanol glass at 90 K (by UV detection and product analysis) and of both **2a** and **2b** in Ar matrices at 15 K (by UV and IR detection). Furthermore, we examined the properties and the reactivity of both nitrenes by comprehensive quantum chemical calculations. As will be shown, the results revealed some new facets of the chemistry of both states of phenylnitrenes and indicated the limits for the formation of heterocycles through intramolecular reactions, i.e., the most useful synthetic application of phenylnitrenes.[10]

2. Results and Discussion

2.1. Experimental Studies. Pyrazolylphenylnitrene 2a. Irradiation of 1×10^{-4} M azide **1a** in argon-flushed EtOH at room temperature gave the amine **3a**, the azo derivative **4a**, and pyrazolo[1,2-*a*]benzopyrazole **5a** in yields of 39, 18, and 24%, respectively, at >95% conversion (cf. Scheme 2; preparative experiments for the isolation of the products were done on 5×10^{-3} M solutions). In the presence of 0.1 M diethylamine (DEA), the yields of products **3a** and **4a** were almost unchanged, but that of **5a** was lowered in favor of two products incorporating the amine in 30% combined yield. These were identified as the tautomeric 2-diethylamino-7-pyrazolylazepines **6a** and **6a′** (see the experimental part).

Irradiation of **1a** at 254 nm in an EtOH glass at 90 K until >90% bleaching led to conspicuous new absorptions at ca. 330 and 530 nm (see Figure 1a), assigned to ^{3}**2a** in view of the similarity to other triplet phenylnitrenes (more stringent evidence is reported below). On melting the glass, UV and HPLC showed that **4a** was the main product, accompanied by some amine **3a** and a trace of heteropentalene **5a** (Scheme 2).

Upon irradiation of the glass containing ^{3}**2a** at >450 nm, the absorption of this transient was replaced by new bands at ca. 220, 300, and 365 nm (the black line in Figure 1b) which remained unchanged after melting the glass. HPLC revealed 20% of **3a**, a small amount of **5a** (absorbing at 365), no **4a**, and, as the main product (55%), a compound not formed at room temperature, to which belonged the bands at 220 and 300 nm. This was an isomer of **2a** (*m*/*e* 157, LC/MS), to which the structure of pyrazolo[1,5-*a*]benzimidazole **7** (Scheme 2) was assigned, on the basis of the similarity of its UV spectrum to that of carbazole. Further evidence to support this assignment will follow below.

Irradiation (254 nm) of **1a** in an Ar matrix at 12 K gave a similar spectrum, with considerably more fine structure (the red line in Figure 1c). Bleaching at >515 nm led to the disappearance of the bands above 370 nm, of the system at 310−360 nm, and of a sharp peak at 260 nm (the blue line in Figure 1c), while the small peak at 367 nm and the sharp bands at 305/299/293 nm, which all belong to **5a**, increased. The correspond-

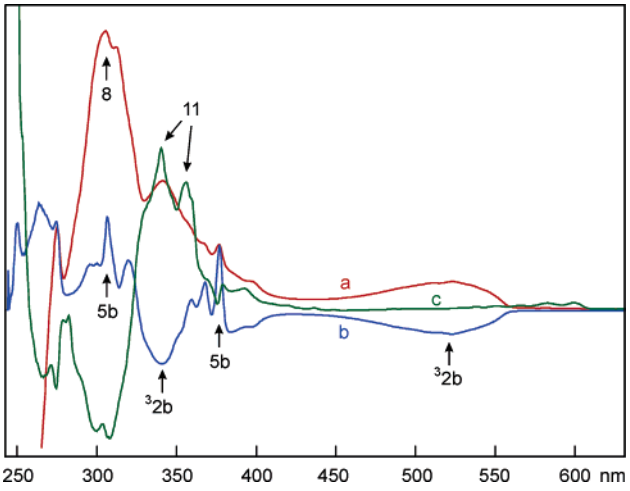

Figure 3. Difference spectra for (a) the formation (254 nm photolysis of azide **1b**, red line) and (b) the >525-nm bleaching of nitrene **2b** (blue line) in an Ar matrix at 12 K. Spectrum c (green line) relates to subsequent irradiation at 313 nm, which leads to dehydrogenation of dihydroquinoxaline **8** (see the text).

ing IR difference spectra (Figure 2) showed that most of the peaks generated at 254 nm matched those calculated for ^{3}**2a** (bottom of Figure 2a). These features disappeared upon bleaching at >515 nm, while some peaks already present after reaction of **1a** (marked with asterisks in Figure 2a) increased (Figure 2b). Comparison with the calculated IR spectrum of **7** (top of Figure 2) confirmed the assignment to this species; The IR spectra showed also that very little **5a** was formed.

Subsequent photolysis at 365 nm (not shown) converted **5a** into triazasemibullvalene **9a** (Scheme 3) in a reaction that can be reverted at 313 nm,[29] while **7** was slowly converted to a species weakly absorbing at 610 nm, tentatively identified as radical **10** (Scheme 3) due to the close similarity to the *N*-carbazolyl radical.[30]

Dimethylpyrazolylphenylnitrene 2b. The previously reported photochemistry of the dimethyl derivative **2b** in EtOH[26,31,32] gave heteropentalene **5b** as almost the only product at room temperature, but in the presence of DEA, two regioisomeric adducts, 2-diethylamino-3-pyrazolylazepine **6b″** (22%) and 2-diethylamino-7-pyrazolylazepine (**6b**, 3%), were formed, along with low yields of amine **3b** and azo compound **4b** (cf. Scheme 2). The triplet nitrene (^{3}**2b**) was again cleanly produced at 90 K and melting of the glass gave **4b**, though further irradiation at >450 nm gave dihydropyrazoloquinoxaline **8**, with a minor amount of **5b**.

We now carried out the reaction in an Ar matrix at 12 K, reproducing the UV/vis absorptions at 340 and 530 nm of ^{3}**2b** (Figure 3a) and strengthening the identification by comparing the corresponding IR spectrum obtained with that calculated for ^{3}**2b** (Figure 4). An intense band at ca. 300 nm belonging to **8** (comparison with an authentic sample) and a weak indication of **5b** at 365 nm were also observed. The latter bands increased markedly upon >515-nm bleaching of ^{3}**2b**, along with the 305-nm peak of **5b** (Figure 3b).

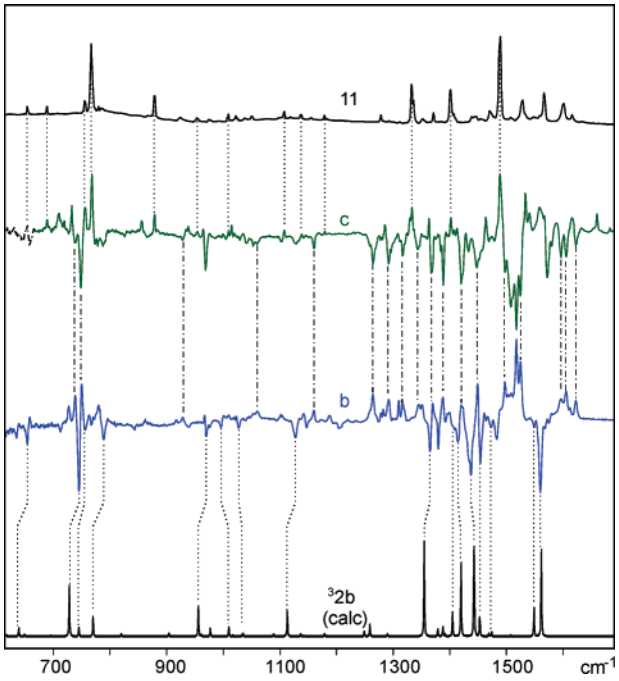

Figure 4. IR difference spectra corresponding to spectra b (blue line) and c (green line) in Figure 3. The bands that decrease in b are correlated with those of the simulated spectrum of nitrene ^{3}**2b**. (B3LYP/6-31G* calculation of most stable conformer) at the bottom. Peaks that rise in b and decrease in c (dashend lines) are due to dihyroquinoxaline **8**, while those that rise in c are correlated with the IR spectrum of quinoxaline **11** at the top.

Subsequent irradiation at 313 nm (traces c in Figures 3 and 4) bleached the UV and IR bands of **8** and gave a band at ca. 350 nm and IR peaks (pointing up in Figure 4c) attributed to quinoxaline **11** by comparison with an authentic sample (top of Figure 4). A small band at 1886 cm^{-1} also rose, indicating the formation of a dehydroazepine, recognized as **15b** rather than regioisomeric **16b** by comparison with the calculated spectrum (see Supporting Information). On the other hand, we had previously shown that 365-nm bleaching of **5b** gives triazasemibullvalene **9b**, in a reaction that is photoreversible at 313 nm.[29]

Summing up, at room temperature heteropentalenes **5** are formed from the singlet nitrenes as the only isolated products (72% from **1b** and 24% from **1a**, paths *a* and *e*, respectively in Scheme 4). Triplet nitrene products (after ISC, path *b*) are abundant from **1a** (**3a** and **4a**, together 54%), while they are absent from **1b** (Scheme 4). In the presence of DEA, aminoazepines are formed through trapping of dehydroazepine **16** (via path *d*, that followed by most *o*-substituted phenylnitrenes)[33−37] in the case of **1b** and trapping of **15** (via path *c*, as expected e.g. for *o*-cyanophenylnitrene)[4] in the case of **1a**. As in previous cases,[21] addition of DEA was found to slightly enhance the yield of tripled derived products, perhaps because it increases the overall yield of isolable products.

Triplet nitrenes are formed both in EtOH glasses and in Ar matrices, but subsequent visible light irradiation gives contrasting results (Scheme 3). ^{3}**2a** attacks the pyrazole π-system to give **7** (presumably via **17**, path *e* in Scheme 4), while yielding only a trace of **5a** and no dehydroazepines. With ^{3}**2b** the main product is **8**, which arises by H-abstraction from the methyl group presumably via diradical **18** (path *f*), with a significant (1 to 5) proportion of **5b** and a small amount of dehydroazepine

(29) Carra, C.; Bally, T.; Jenny, T. A.; Albini, A. *Photochem. Photobiol.* **2002**, *1*, 38.
(30) Levya, E.; Platz, M. S.; Niu, B.; Wirz, J. *J. Phys. Chem.* **1987**, *91*, 2293.
(31) Albini, A.; Bettinetti, G.; Minoli, A. *J. Am. Chem. Soc.* **1991**, *113*, 6928.
(32) Albini, A.; Bettinetti, G.; Minoli, G. *Heterocycles* **1995**, *40*, 597.

Scheme 3. Products Obtained after 254-nm Photolysis of Azides **1a** and **1b** in Ar at 12 K

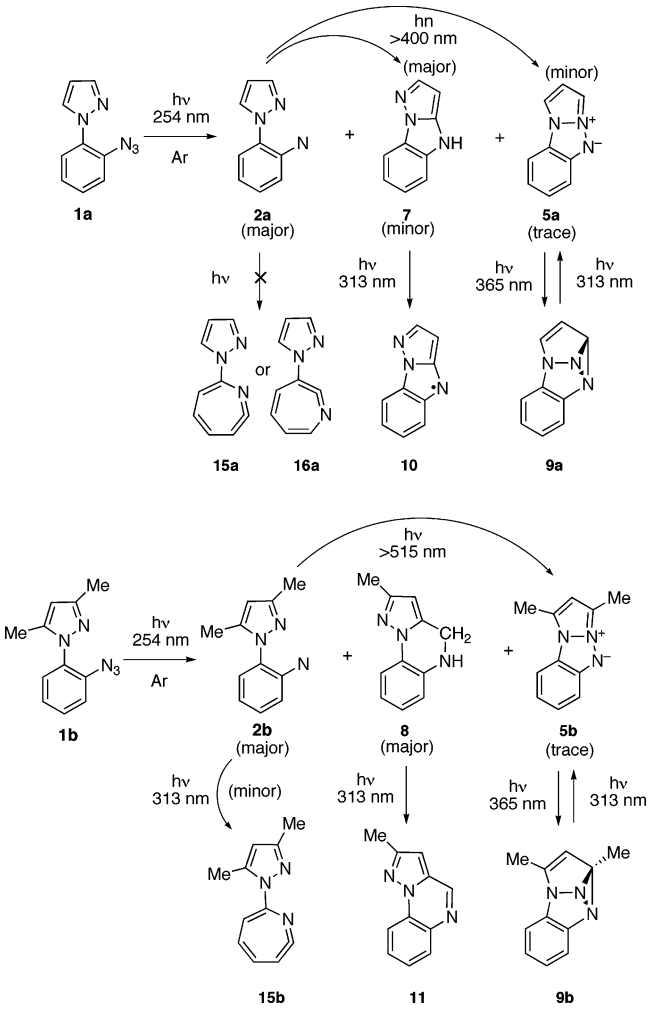

15b. In Ar matrices, further photochemistry of the above products is observed, namely reversible rearrangement of **5a**,**b** to **9a**,**b** and hydrogen loss from **7** to give **10** and from **8** to give **11**.

2.2. Computational Study of the Conformation of Azides and Nitrenes. The above experiments show that intramolecular attack of the pyrazole nitrogen by the singlet nitrene is more efficient (and competes more effectively with ISC to the triplet) in **2a** than in **2b**, a finding for which we considered the following rationalizations:

(a) Cyclization to the heteropentalenes **5** requires that the pyrazole N lone pair faces the nitrene N atom. The percentage of this conformation may differ in **2a** and **2b**.

(b) The nucleophilicity of the pyrazole N lone pair is increased by the methyl groups.

(c) Intersystem crossing may be faster in **2a** than in **2b**, thus siphoning away singlet nitrene more rapidly than it can cyclize to **5a**.

All of the above factors may be operative simultaneously, but only the first two are amenable to computational exploration.

Scheme 4. Summary of the Observed Decay Paths of Nitrenes 2

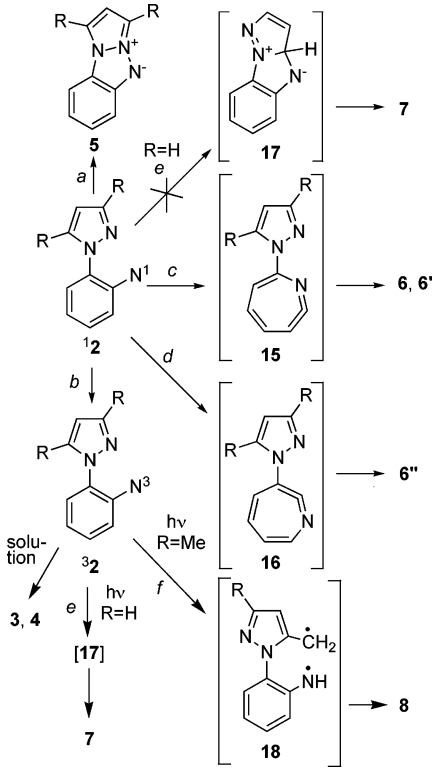

Thus we analyzed the conformational surfaces of azides **1** and nitrenes **2** by calculations.

Parent System 1a/2a. Full geometry optimizations (B3LYP/6-31G*) led to four conformational minima in the case of **1a** (structures in the top row of Figure 5), pairwise related by the conformation of the azide (**1a** and **1a′**) and the pyrazolyl groups (denoted **NH** or **NN**), respectively, and distinguished by the dihedral angle between the phenyl and the pyrazole rings. We calculated that 93% of the parent azide is present as the **1a**(**NH**) conformer at room temperature,[38] suggesting that, unless deazotation involves rotation around the phenyl−pyrazole bond, the N atom is mainly facing a pyrazole C−H bond in the incipient nitrene.

The corresponding (optimized) structure of *triplet* nitrene (^{3}**2a**(**NH**) in Figure 5) is clearly favored over the other conformation, ^{3}**2a**(**NN**), where the nitrene N atom faces the pyrazole N lone pair, presumably due to a stabilizing interaction between the pyrazole H-atom vicinal to the nitrene N (distance < 2 Å) in the former and to a repulsive interaction between the two N atoms (indicated by deviation from planarity) in the latter conformation. The Arrhenius activation energy [$E_a = \Delta H(T)^+RT$] for their conversion is 6.66 kcal/mol at room temperature (6.56 kcal/mol at 77 K), i.e., the two conformations cannot interconvert at 77 K, let alone at 12 K, once they are formed.[39]

(33) Berwick, M. A. *J. Am. Chem. Soc.* **1971**, *93*, 5780.
(34) Sundberg, R. J.; Sutar, S.; Brenner, M. *J. Am. Chem. Soc.* **1972**, *94*, 513.
(35) Lamara, K.; Redhouse, A. D.; Smalley, R. K.; Thompson, J. R. *Tetrahedron* **1994**, *50*, 5515.
(36) Levya, E.; Sagredo, R. *Tetrahedron* **1998**, *54*, 7367.
(37) Karney, W. L.; Borden, W. T. *J. Am. Chem. Soc.* **1997**, *119*, 3347.

(38) The B3LYP/6-31G*-calculated Arrhenius activation energies for the rotation of the pyrazolyl groups are 2.76 kcal/mol (**1a**(**NH**) → **1a**(**NN**)) and 0.52 kcal/mol (**1a′**(**NH**) → **1a′**(**NN**)) at 298 K, and those for rotation of the azide group are 4.31 kcal/mol (**1a**(**NN**) → **1a′**(**NN**)) and 3.68 kcal/mol (**1a**(**NH**) → **1a′**(**NH**); full details are given in the Supporting Information). Thus, the four conformations of azide **1a** equilibrate rapidly at room temperature.
(39) In addition, a CASSCF optimization of the first excited triplet state of **2a** showed that the bond between the phenyl and the pyrazole ring *shortens* and that the excited triplet shows no tendency to undergo rotation around that bond (Carra, C., unpublished results). Hence, no conformational change is expected to occur on bleaching of ^{3}**2a**.

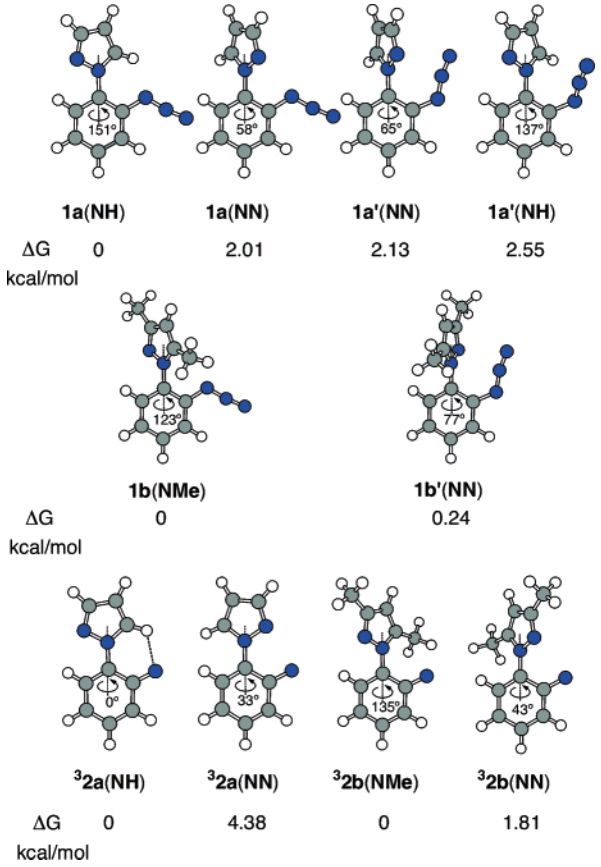

Figure 5. Conformers of azide **1a** (top line), azide **1b** (middle line), and of the triplet nitrenes ^{3}**2a** and **2b** (bottom line). The numbers inside the phenyl rings denote values of the phenyl−pyrazolyl dihedral angle. Structures and ΔG values are from B3LYP/6-31G* calculations.

Table 1. Relative Energies[a] of the Two Conformers of Nitrene **2a** in Its Singlet and Triplet State, Activation Energies for Their Interconversion, S/T Gaps, and Some Critical Geometry Parameters

	B3LYP	CASPT2[b,c]	S/T gap[d]	ω[c,e]/ deg	r(C−N)/ Å[c]	r(N···H)/ Å[c]
^{3}**2a(NH)**	(0)	(0)	−	0	1.338	2.233
TS	6.90	5.45	−	93.9	1.349	−
^{3}**2a(NN)**	4.43	3.21	−	129.0	1.348	−
^{1}**2a(NH)**	−	(0)	17.74	0	1.256	2.218
TS	−	8.60	20.88	91.8	1.272	−
^{1}**2a(NN)**	−	6.32	20.92	130.3	1.272	−

[a] In kcal/mol. [b] Based on (14,12) CASSCF calculations; for details, see the Methods section. [c] At the (14,12) CASSCF geometries. [d] Singlet/triplet gap from CASPT2 calculations; E(S) > E(T). [e] Dihedral angle C−C−N−C between the phenyl and the pyrazole rings.

DFT methods do not yield meaningful results for *singlet* ^{1}**2a**, due to the open-shell nature of this species and the resulting multideterminantal nature of its wave function,[5,19] so we resorted to the CASSCF/CASPT2 methodology to calculate both spin states of nitrenes **2a**. As shown in Table 1, the **NN** conformers are consistently less stable than the (planar[40]) **NH** conformers, presumably due to a repulsive effect of the pyrazole N lone pair.[41] However, the energy difference is nearly twice as high in the singlet than in the triplet state. As Borden et al. have explained,[19] the triplet and the (open-shell) singlet states of phenylnitrenes have a comparable electronic structure, but while in the former the Coulombic repulsion between the unpaired electrons is minimized "inherently" by the Pauli exclusion principle, an increased spatial separation is required in the singlet to achieve a similar effect. As one of the electrons occupies an in-plane p-AO of the N atom, the other one must be in a π-orbital that is localized at the far end of the phenyl ring. Thus, singlet phenylnitrene resembles a cyclohexadienyl radical linked to an iminyl radical (short C═N bond), whereas the triplet rather resembles more a benzyl radical (longer C−N bond).

This holds also for **2a** (see Table 1), with the additional consequence that the nonbonded N···H distance in the **NH** conformer is shorter in the singlet, even though the C−N bond is longer (and hence the nitrene N atom is closer to the pyrazole H) in the triplet. This attractive interaction between the nitrene N and the vicinal pyrazole H atoms makes the singlet−triplet gap shrink from almost 21 kcal/mol in the **NN** conformer (or in the transition state (TS) between the two conformers), to 17.7 kcal/mol in the **NH** conformer.[42] This N···H interaction may also hinder N−C bond formation by attack on the pyrazole π system (see below).

The two rotamers[43] readily equilibrate at room temperature (although the **NN** concentration is tiny), and thus, the fate of ^{1}**2a** depends on the relative rates of the competitive decays rather than on its native conformation. In contrast, at 90 or 10 K, ISC precludes reactions from ^{1}**2a** and the conformers do not interconvert; thus the products are dictated by the conformation of the starting azide and of the incipient nitrene. Indeed, the main product under these conditions is pyrazolobenzimidazole **7**, only accessible from the **NH** conformer.

Dimethyl Derivative 1b/2b. To our surprise a systematic conformational search of azide **1b** revealed only two minima, **NN** and **NMe**,[44] with the conformers in a ca. 60:40 mixture at room temperature according to their B3LYP free energy difference.[45] Since the two aromatic rings are nearly perpendicular in both structures, this imposes little bias on the nascent nitrene. In the triplet nitrene, ^{3}**2b**, the free energy difference between the two conformers is much smaller than in ^{3}**2a**, and the barrier for their interconversion is much lower (3.20 or 1.12 kcal/mol, respectively, at 298 K), since they deviate already by about 50° from planarity.

All attempts to find a CASSCF potential energy minimum corresponding to the **NN** conformer of ^{1}**2b** converged to the **NMe** conformer, suggesting that decay to the latter (Table 2) is barrieless in this case.

(40) CASSCF predicts nonplanar equilibrium conformations for the **NH** conformation, both in triplet (dihedral angle 56.7°) and singlet **2a** (dihedral angle 57.5°). In both cases CASPT2 favors, however, a planar conformation of C_s symmetry, so only this conformation is considered here.

(41) Note that the CASSCF dipole moment of **2a**(**NN**) is much higher than that of **2a**(**NH**) (4.3 vs 1.7 D). Thus, the energy difference between the two conformers may be strongly attenuated in polar solvents, e.g. ethanol.

(42) The extent of this effect depends quite strongly on the size and the nature of the active space in the CASSCF calculations. Removing the σ lone pair on the nitrene N atom from the active space does not affect the energy difference between the two conformers in the triplet state but reduces that difference in the singlet state from 6.4 to 4.5 kcal/mol (and increases the S/T gap in the H-bonded conformer to 20.4 kcal/mol, only 1 kcal/mol less than in the other conformer).

(43) The transition states were found to be stationary points in a saddle point search. Unfortunately, we were unable to perform frequency calculations at the CASSCF(14,12) level to ascertain the nature of these stationary points and to obtain vibrational data for thermal corrections. However, the transition state found for the triplet nitrene looks very similar to that found (and characterized) by B3LYP, so we have reason to be confident that we have actually located true saddle points also by CASSCF.

(44) To convince ourselves that we had not missed a secondary minimum, we carried out relaxed scans of the dihedral angle, the results of which are summarized in Figure S1 of the Supporting Information.

(45) The B3LYP/6-31G* calculated Arrhenius activation energy for the interconversion of the **NMe** and the **NN** conformer is 3.71 kcal/mol at 298 K (full details are given in the Supporting Information). Thus, the two conformations of ^{1}**2b** equilibrate rapidly at room temperature.

Table 2. Relative Energies[a] of the Two Conformers of Nitrene **2b** in Its Singlet and Triplet State, Activation Energies for Their Interconversion, S/T Gaps, and Some Critical Geometry Parameters

	B3LYP	CASPT2[b,c]	S/T gap[d]	ω[e]/deg	r(C–N)/Å
^{3}**2b(NMe)**	(0)	(0)	−	63.7[b]	1.347[b]
TS	3.33	−	−	95.7[f]	1.327[f]
^{3}**2b(NN)**	2.13	2.40	−	108.0[b]	1.348[b]
^{1}**2b(NMe)**	−	−	21.25	130.3[b]	1.272[b]

[a] In kcal/mol. [b] Based on (14,12) CASSCF calculations; for details, see the Methods section. [c] At the (14,12) CASSCF geometries. [d] Singlet/triplet gap from CASPT2 calculations; $E(S) > E(T)$. [e] Dihedral angle C−C−N−C between the phenyl and the pyrazole rings. [f] At the B3LYP geometry.

Indeed, conformational preference appears to play no role at room temperature, where **5b** is virtually the only product, whereas at 90 K its yield is reduced to 1%. Subsequent irradiation of the nitrene in matrices does yield 10% **5b**, but most of the nitrene **2b** decays by H-abstraction from the proximate methyl group, reflecting the conformational preference of the **NMe** over the **NN** conformer, both in the azide and in the nitrene (cf. Figure 5).

It remains to note that the singlet/triplet gap in **2b** as well as the C−N bond length in ^{1}**2b** are very similar to the values found in the **NN** conformer of **2a**, demonstrating that the **NH** conformer of **2a** is the exceptional case, for the reasons discussed above.

2.3. Competitive Reactions of Singlet Nitrenes: Computational Studies. The above data on the **NN** vs **NH** (**NMe**) equilibria offer a rationalization for the results obtained in matrices, but in general, the competing intramolecular decay paths of Scheme 4 must also be taken into account. Thus, we carried out calculations of the activation energies for attack at the nitrogen or carbon atom of the pyrazole ring (paths *a*, *e*), for insertion into the methyl group (*f*), and for cyclization to benzoazirines (*c*, *d*) for the conformers of both nitrenes. *Inter*molecular reactions of the triplets, such as H abstraction from the solvent and dimerization to give azo compounds, were not considered. The results of CASSCF(14,12)/CASPT2 and B3LYP calculations are presented schematically in Figures 6 and 7 (precise numbers are given in the Supporting Information).

We[9] and others[5] have recently found that, although singlet nitrenes are not amenable to DFT calculations due to their high diradicaloid character, the transition states for their "chemical" decay processes may be modeled fairly well (compared to CASSCF structures and CASPT2 energies) if α and β-electrons are *not restricted* to occupy the same orbitals in the wave function that models the density.[46] We found the same to be true in the present case, at least as long as spin contamination (as indicated by the expectation value of the $\hat{\mathbf{S}}^2$ operator) remains moderate, which is the case for the transition states leading to azirines (but less so for those leading to **5a** and **17**, where $\langle \hat{\mathbf{S}}^2 \rangle = 0.65$ and 0.86, respectively). To be able to compare the results of the two types of calculations, we "anchored" the B3LYP numbers on the triplet state of the **NH** conformer of **2a** or the **NMe** conformer of **2b**, respectively, adding the CASPT2 singlet−triplet gap to arrive at a common origin of the energy scale (=the most stable conformer of the *singlet* nitrene). As it appears from Figures 6 and 7, the activation barriers for the three intramolecular reactions of ^{1}**2a** are all within ca. 5 kcal/mol at the CASPT2 level, and those for ^{1}**2b** lie even closer, thus we expect that these processes compete at room temperature.

The Benzoazirine−Dehydroazepine Path. For the cyclizations to azirines **13a** and **14a**, separate reaction paths, leading to separate conformers of the products, were found for the two conformers of singlet ^{1}**2a**. Those originating from the more stable **NH** conformers (right-hand side of Figure 6) lead to the more stable **NH** conformers of the azirines over lower barriers compared to the less stable **NN** conformers (left-hand side). Thus, we will restrict the discussion to the former intermediates.

Interestingly, formation of the less stable azirines **14a** involves lower barriers than those for formation of their more stable isomers, **13a**. The pyrazole substituent stabilizes azirines **13a** vs isomers **14a**, but it has the opposite effect (due to steric hindrance) on the transition state for cyclization *toward* itself. A similar, though less pronounced effect was seen in *o*-biphenylnitrene,[5] where it did, however, not lead to a curve crossing. As in that case, the DFT activation energies for cyclization to azirines are generally higher than those found at the CASPT2/CASSCF level, but the relative energies of the transition states are similar.

As with other phenylnitrenes,[3,4,19,37] azirines **13a** and **14a** readily open to didehydroazepines **15a** and **16a**, respectively. According to B3LYP calculations, the isomers **15a** are more stable than **16a**, especially in the **NH** conformers, where a hydrogen bond ($R_N\cdots H = 2.53$ Å) contributes probably to the extra stabilization. There is no steric effect in this step (which follows the Bell−Evans−Polanyi principle), but the effect on the first step influences the *overall* reaction from ^{1}**2a** to the didehydroazepines, which leads more rapidly to **16a** than to the more stable **15a**. Once formed, **15a** must overcome a considerable barrier to revert to ^{1}**2a** (E_a(B3LYP) = 21.7 kcal/mol at 298 K),[47] whereas equilibration of **16a** with ^{1}**2a** is expected to be rapid at room temperature (E_a(B3LYP) = 9.9 kcal/mol at 298 K),[47] allowing a path back to **15a**. Experimentally, only azepines **6a**/**6a′** (from the trapping of **15a** by DEA) are formed at the expense of **5a**. Apparently, the peculiar structure of **15a**, with its intramolecular H bond, makes it more reactive toward amines.

In the dimethyl derivative (Figure 7), the cyclizations to azirines are predicted to be more exothermic than in the parent compound, and the barriers decrease by over 5 kcal/mol for both modes,[48] although the *difference* in activation energies for cyclization toward and away from the pyrazole ring remains at 5.5 kcal/mol. Apparently, the methyl groups on the pyrazole exert a stabilizing electronic effect on the transition states (even in **14b** where there is no steric effect) and attenuate the difference in stability between the isomers **13** and **14**.

The ensuing ring-opening reactions are less affected by the methyl groups: that of **13b** is more exothermic by ca. 2 kcal/

(46) Hrovat, D. A.; Duncan, J. A.; Borden, W. T. *J. Am. Chem. Soc.* **1999**, *121*, 169.

(47) Note that this number is not identical to the energy difference between the corresponding stationary points in Figures 6 and 7 because the Arrhenius activation energy, E_a, corresponds to an *enthalpy* difference (augmented by *RT* for a unimolecular reaction).

(48) One may argue that these differences between the parent system and the dimethyl derivative come about by an error in the calculation of the singlet/triplet gap. However, to explain a 5 kcal/mol difference in activation energies would require the *relative* S/T gap of the parent system and the dimethyl derivative to be in errror by a similar amount. In the absence of H-bonds, the S/T gaps of the two compounds are calculated to be about the same (21 ± 0.2 kcal/mol), which is reasonable. Thus we believe that the differences in exothermicities and activation barriers for cyclization to azirines are not artifactual.

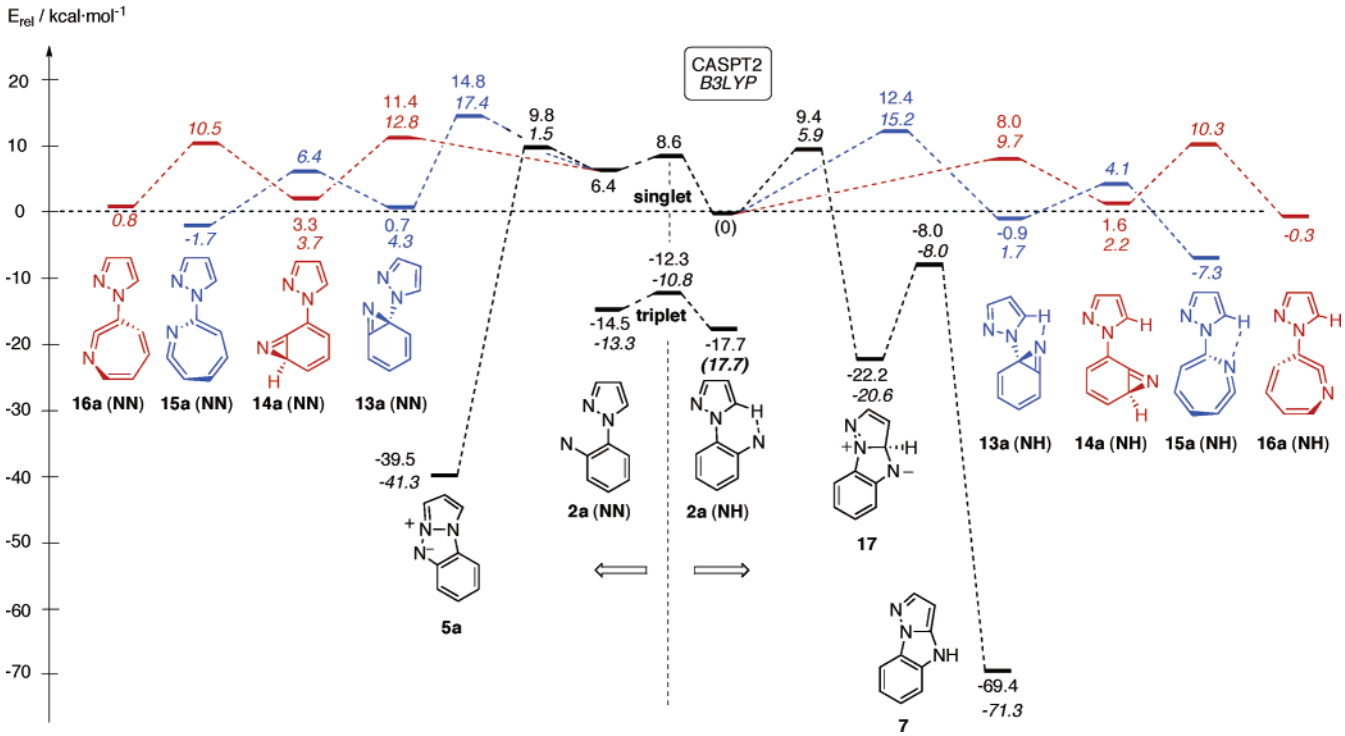

Figure 6. Potential energy surface on which the different rearrangements of nitrene **2a** take place. The B3LYP (normal font) and CASPT2 relative energies (italic) are made to coincide for the **NH** conformer of ^{3}**2a**. Adding the CASPT2 singlet−triplet gap for this species leads to the origin of the energy scale.

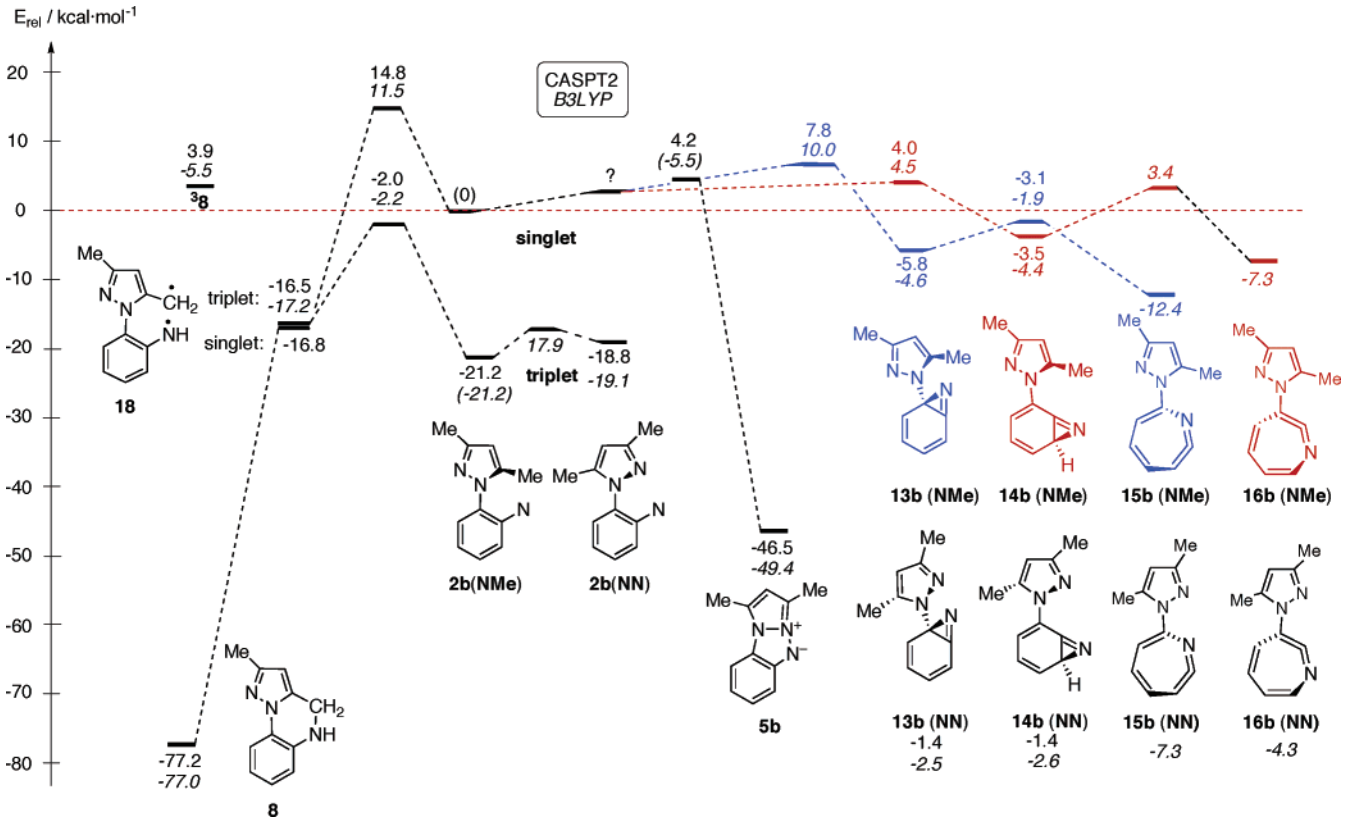

Figure 7. Potential energy surface on which the different rearrangements of nitrene **2b** take place. The B3LYP (normal font) and CASPT2 relative energies (italic) are made to coincide for the **NMe** conformer of ^{3}**2b**. Adding the CASPT2 singlet−triplet gap for this species leads to the origin of the energy scale.

mol with a barrier lowered by ca. 3 kcal/mol and that of **14b** is less exothermic but proceeds over a slightly lowered barrier. Overall, the less stable dehydroazepine **16b** is again predicted to be formed more rapidly than its more stable isomer **15b**, although the energy difference is smaller than in ^{1}**2a**. The barrier for reversal of **15b** to ^{1}**2b** is twice as high (E_a(B3LYP) = 20.9 kcal/mol at 298 K)[47] than that for **16b** (E_a(B3LYP) = 9.7 kcal/mol at 298 K).[47] Experimentally, trapping of **16b** predominates over that of **15b** and this corresponds to what is observed with most *o*-substitued phenylnitrenes, which cyclize "away" from

the substituent,[4,10,33−37] just as **2b** does, singling out the abnormally easily trapped **15a** (see above).

In the absence of diethylamine, the didehydroazepines form a reservoir from which singlet nitrenes ^{1}**2** are replenished. Indeed, evidence from flash photolysis studies supported that a part of **5** is formed in a slow reaction,[31] thus supporting such an equilibrium. Other products may be obtained by irreversible processes if their rates are competitive with that for intersystem crossing to ^{3}**2** (path *b* in Scheme 4). Indeed, the activation barriers for thermal reactions of the singlet nitrenes are generally lowered by 4−5 kcal/mol on bismethylation of the pyrazole ring, thus explaining why at room temperature ISC is negligible in ^{1}**2b**, whereas it predominates in ^{1}**2a** (70% in the absence of the amine, 60% in its presence).

Attack on the Pyrazole Ring. According to the (gas phase) CASPT2 calculations, attack of nitrene ^{1}**2a** on the pyrazole π-system (yielding **17** and then **7**) should be slightly favored over attack on the N lone pair (yielding **5a**). The opposite result obtained in solution is explained by the much higher dipole moment of the transition state leading to **5a** (3.4 D) compared to that leading to **17** (1.5 D). This favors formation of **5a** in polar solvents, while the above-mentioned N···H interaction with the pyrazole H atom in ^{1}**2a** disfavors formation of **17** in solution. The latter compound is the main product obtained on photoexcitation of ^{3}**2a** in frozen matrices, but this results from the fact that the nitrene N-atom faces the CH bond of the pyrazole in the predominant conformation.

Formation of **5a** from ^{1}**2a** is predicted to involve an activation energy that is lower by ca. 3 kcal/mol than that for cyclization to azirine **13a** (and hence to **6a**) at the CASPT2 level. However, CASPT2 calculations are known to overestimate the latter barrier by 2−3 kcal/mol.[5,49] Accordingly, the two processes compete in solution, although ISC to the triplet funnels away two-thirds of the nitrene, leading to a low yield of **5a**.

In the case of ^{1}**2b**, the much greater efficiency of ring closure to yield **5b** is explained by the lower calculated barrier. This is in part due to the greater exothermicity (by 7−8 kcal/mol) in forming **5b** rather than **5a** (a product effect, not expressed in the position of the transition state, however, since the N···N distance at the transition state is 2.07 Å in both cases) and more importantly due to the enhanced nucleophilicity of the pyrazole N lone pair caused by the methyl groups. Indeed, B3LYP calculations on pyrazole show an increase of the energy of the N lone pair by 0.2 eV upon 3,5-dimethylation.

Intramolecular Hydrogen Abstraction. The only other decay process of nitrene **2b**, H abstraction from the proximate pyrazole methyl group, encounters a much higher barrier. Indeed, **8** is not formed upon direct irradiation of **1b** at room temperature, whereas ^{1}**2b** decays through path *a* (Scheme 4). However, some **8** is formed by thermal decomposition at 143 °C of **1b** (15%), via the triplet nitrene by photosensitization of **1b** in solution (10%),[31,32] and from the relaxed triplet nitrene in an EtOH glass at 90 K (10%), although the calculated thermal barrier is not negligible (E_a(B3LYP) = 15.6 kcal/mol at 298 K).[47] Thus, our calculations document the well-known "lazy" character of phenylnitrene triplets toward H-abstraction,[16,26−28,32] which is apparently not "cured" by making the reaction intramolecular as in ^{3}**2b**.

However, this "laziness" can be overcome by excitation of ^{3}**2b** in a low-temperature matrix, where **8** is formed as the major product (a little unreacted nitrene abstracts hydrogen from the solvent and gives 6% **3b**).[50] This is reasonable, because the lowest excited state of ^{3}**2b** lies at ca. 30 kcal/mol on the energy scale in Figure 7, i.e., well above the barrier leading to **8**, and this process is further favored by the predominant **NMe** conformation of the triplet nitrene.[51] The intramolecular reaction with the methyl group is diagnostic, because, in the absence of a specific target for radical attack, excitation of the immobilized triplet nitrene apparently leads back to the *singlet* surface, as indicated in the formation of dehydroazepine from phenylnitrene[19] and carbazole from *o*-biphenylnitrene.[5] Correspondingly, in the present case a trace of **15b** and some **5b** are formed from ^{3}**2b**, and **17** is the main product from nonmethylated ^{3}**2a** by irradiation in the matrix.

The further reactions in matrices are secondary reactions. The reversible photorearrangement **5** → **9** has been previously reported,[29] while hydrogen loss from benzimidazole **7** and dehydrogenation of dihydroquinoxaline **8** are homolytic processes caused by the lack of energy dissipation channels in the Ar matrix.

3. Conclusions

Nitrene **2b** has been proposed almost 30 years ago as a mechanistic probe designed to distinguish the electrophilic chemistry of the incipient singlet phenylnitrene from the expected radical chemistry of its triplet ground state through intramolecular reactions, and thus to rationalize and direct the use of these intermediates. In the meantime, work by several groups has documented through elaborate experiments and calculations how the cyclization to benzoazirines hampers the synthetically desirable intermolecular chemistry of singlet phenylnitrene. A classical intramolecular electrophilic reaction, that of *o*-biphenylnitrene, has also been theoretically studied in detail recently.[5]

Considering nitrenes **2a** and **2b** adds a degree of complexity because *two* modes of intramolecular electrophilic attack (*a* and *e* in Scheme 4) compete with two cyclizations (paths *c* and *d*) and with intramolecular radical attack (path *f*). Furthermore, conformational equilibria must be taken into account. Indeed, the product distributions shown in Schemes 2 and 3 and the potential energy surfaces in Figures 6 and 7 are quite intricate, but it has been possible to explain the chemistry observed as a complex function of the conformational distribution and the barriers encountered on the various decay paths, thus evidencing some key aspects.

In particular, it is clarified that attack on the pyrazole N lone pair differs from attack on the π system in that it involves a more polar transition state. The former process predominates

(49) Karney, W. L.; Borden, W. T. *J. Am. Chem. Soc.* **1997**, *119*, 1378.

(50) Photoinduced *intermolecular* H-abstractions of triplet nitrenes are known, cf.: Levya, E.; Munoz, D.; Platz, M. S. *J. Org. Chem.* **1989**, *54*, 5938.

(51) The primary product of hydrogen abstraction from the methyl group is biradical **18**. This turns out to be an interesting species, because it has an open-shell singlet ground state that is almost degenerate with the corresponding triplet state. The corresponding closed-shell singlet state (which is what is obtained in a DFT calculation) corresponds to a polyeneimine and lies vertically about 22 kcal/mol above the open-shell singlet ground state of **17**. However, on geometry optimization that state ends up only ca. 5 kcal/mol above that state (all CASSCF/CASPT2 results). We did not succeed in finding a transition state for the cyclization of the open-shell singlet state to dihydroquinoxaline **8** (all attempts to shorten the distance betweeen the two radical centers resulted in collapse to **8**), so we assume that this process is essentially barrierless.

in solution, highlighting the electrophilic character of the singlet nitrene, as seen in the increased efficiency with the more nucleophilic dimethylpyrazole, a requisite for overcoming ISC on the triplet. Attack to the pyrazole π system is a more complex reaction, similar to what has been found with *o*-biphenylnitrene,[5] and is obtained by photoexcitation of the nitrene in a matrix.

As for triplet phenylnitrene, the "lazy" character of this species has for the first time been documented through a computational study, indicating also that the *excited* triplet is a good hydrogen abstractor. Finally, in matrices, the conformational equilibration of the *o*-pyrazole substituent is suppressed and the phenylnitrene photochemistry is dictated by the conformation of the nascent nitrene.

As for the general rationalization of the chemistry of phenylnitrenes, Platz[16] previously pointed out that the rapid cyclization to benzoazirine (finally leading to tars and/or to ISC) makes the *intermolecular* chemistry of the singlet nitrene synthetically less useful than that of phenylcarbene. The present study shows that such cyclization competes even with *intramolecular* attack to a lone pair. Formation of a benzofused heterocycle such as **5** can compete with other decay processes only when the nucleophilic site is further activated. The limits to the use of (hetero)arylphenyl azides for the synthesis of carbazole analogues are clearly stringent.

Experimental and Theoretical Section

General Information. NMR spectra were run on a Brucker 300 instrument and are reported in $CDCl_3$ with TMS as an internal standard; attributions are based on the appropriate double irradiation experiments. IR spectra were collected on a Perkin-Elmer Partaon 1000 spetrophotometer and mass spectra on a Finnigan LCQ instrument. Ethanol (95%) was spectroscopic grade solvent. Column chromatography was performed with silica gel Merck HR 60. The azides were prepared as previously reported.[26]

Preparative Irradiation. Preparative irradiations and chromatographic product separations were carried out as in previous reports.[26] The characterization of photoproducts **3**, **4**, **5**, **6b**, **8**, **9**, and **11** has been previously reported.[21,26,29] The main analytical data for the newly isolated photoproducts are reported below (assignment based on DEPT and NOESY experiments).

3*H*-2-Diethylamino-7-pyrazolylazepine (**6a**): slightly yellow oil: ^{1}H NMR [$(CD_3)_2CO$] δ 1.3 (t, 6H), 3.0 (d, 2H, J = 7 Hz, H_2-3), 3.6 (q, 4H), 5.3 (q, 1H, J = 7 Hz H-4), 6.3 (dd, 1H, J = 2, 2.5 Hz, pyrazole H-4), 6.4 (dd, 1H, J = 7, 9 Hz, H-5), 6.7 (d, 1H, J = 9 Hz, H-6), 7.55 (d, 1H, J = 2 Hz, pyrazole H-5), 8.2 (d, 1H, J = 2.5 Hz, pyrazole H-3), NOE enhancement between the *N*-CH_2 and the 3-CH_2 groups; ^{13}C NMR [$(CD_3)_2CO$] δ 13.2 (CH_3), 31.1 (CH_2, C-3), 43.9 (CH_2), 95.4 (CH, C-6), 105.1 (CH, pyrazole C-4), 109.5 (CH, C-4), 126.3 (CH, pyrazole C-3), 128.4 (CH, C-5), 139.5 (CH, pyrazole C-5); HRMS calcd for $C_{13}H_{18}N_4$ 230.1531, found 230.1528.

7*H*-2-Diethylamino-7-pyrazolylazepine (**6a′**): slightly yellow oil; ^{1}H NMR ($CDCl_3$) δ 1.3 (t, 6H), 3.55(q, 2H), 5.55 (t, 1H, J = 9 Hz, H-6), 5.7 (t, 1H, Hz, H-4), 6.0 (t, 1H, pyrazole H-4), 6.4 (d, 1H, J = 9 Hz, H-7), 6.9 (dd, 1H, J = 7, 9 Hz, H-5), 7.0 (d, 1H, J = 7 Hz, H-3), 7.1 (d, 1H, J = 2, pyrazole H-5), 7.45 (d, 1H, J = 2 Hz, pyrazole H-3); HRMS calcd for $C_{13}H_{18}N_4$ 230.1531, found 230.1527.

3*H*-2-Diethylamino-7-(3,5-dimethylpyrazolyl)azepine (**6b**) was obtained in a chromatographic fraction admixed with **5b**: ^{1}H NMR ($CDCl_3$) δ 1.17 (t, 6H), 2.18 (s, 3H), 2.27 (s, 3H), 2.9 (d, J = 8 Hz, 1H, H-3), 3.41 (q, 4H), 5.11 (q, J = 8 Hz, H-4), 5.88 (s, 1H), 6.21 (d, J = 6 Hz, H-6), 6.44 (dd, J = 6, 8 Hz), H-5); ^{13}C NMR ($CDCl_3$) δ 12.7 (CH_3), 12.9 (CH_3), 13.5 (CH_3), 29.6 (CH_2), 43.4 (CH_2), 103.6 (CH), 106.2 (CH), 110.1 (CH), 128.3 (CH); HRMS calcd for $C_{15}H_{22}N_4$ 258.1844, found 258.1843.

Photolysis in Ethanol Glass. A 1×10^{-4} M solution of azides **1a**,**b** in EtOH (2 mL) in a 1-cm quartz cell was sealed under vacuum after degassing by four freeze−pump−thaw cycles. The cell was inserted into an Oxford DN 1704 liquid nitrogen cryostat fitted with a calibrated ITC4 temperature controller, placed in a Kontron Uvikon UV−vis spectrometer, and illuminated from the bottom by means of a low-pressure mercury arc (Helios Italquartz 15W). In a typical experiment, the solution was frozen to 90 K, irradiated until the azide was fully consumed (ca. 10 min), warmed to room temperature, and evaporated in the dark, and the residue was redissolved in 1 mL of MeCN for HPLC separation with acetonitrile−water mixtures. The product distribution was determined on the basis of calibration curves. In some experiments, samples photolyzed at 254 nm were further irradiated from the side by a focused high-pressure mercury arc (Osram 150 W) through a cutoff filter (>450 nm) for up to 6 h. Under these conditions, a new peak from **1a** and isomeric with it [base peak 158 $(M + 1)^+$] was assigned to **7** in view of the close similarity of its UV spectrum with that of carbazole, and the calibration curve of carbazole was used for estimating the concentration.

Matrix Isolation and Spectroscopy.[52] Crystals of azides **1a** or **2a** were placed in a U-shaped tube immersed into a water bath and connected to the inlet system of a closed-cycle cryostat. While the bath was kept at 10 °C (**1a**) or 18 °C (**1b**), a mixture of high-purity argon and nitrogen (10:1, to improve the optical quality of the matrices) was flowing through the tube at a rate of ≈1 mmol/h and swept the compounds onto a CsI window held at 19 K. A sufficient quantity of the compound accumulated within 2 h. Electronic absorption (EA) spectra (200−1200 nm) were taken with a Perkin-Elmer Lambda 19 instrument and IR spectra with a Bomem DA3 interferometer (1 cm^{-1} resolution) equipped with an MCT detector (500−4000 cm^{-1}). Photolyses were carried out with low-pressure Hg lamps (254 nm) or with high-pressure Hg/Xe lamps using cutoff or interference filters for wavelength selection, as indicated in the text.

Quantum Chemical Calculations. The geometries of all species except the singlet nitrenes were optimized by the B3LYP density functional method[53,54] as implemented in the Gaussian program package,[55,56] using the 6-31G* basis set. All stationary points were characterized by second derivative calculations which served also for the calculation of vibrational spectra. In the calculations of the transition states for cyclization of singlet phenylnitrenes, the density was modeled by a spin-unrestricted wave function, to allow for some open-shell character, a procedure which has proven to give transition state geometries in good accord with the multideterminantal calculations described below.[5,9] Activation energies computed in this fashion are useful if the spin contamination does not exceed a certain degree ($\langle \hat{S}^2 \rangle$ < 0.2). Otherwise, the admixture of high-spin states leads to an artifactual overstabilization, i.e., to an underestimation of activation energies, as was found, for example, for the transition states leading to heteropentalenes **5**.

Excitation energies were evaluated by time-dependent response theory,[57] according to which the poles and the residues of the frequency-

(52) Bally, T. In *Reactive Intemediate Chemistry*; Moss, R. A., Platz, M. S., Jones, M., Eds.; Wiley: New York, 2003.
(53) Becke, A. D. *J. Chem. Phys.* **1993**, *98*, 5648.
(54) Lee, C.; Yang, W.; Parr, R. G. *Phys. Rev. B* **1988**, *37*, 785.
(55) Frisch, M. J.; Trucks, G. W.; Schlegel, H. B.; Scuseria, G. E.; Robb, M. A.; Cheeseman, J. R.; Zakrzewski, V. G.; Montgomery, J. A.; Stratmann, R. E.; Burant, J. C.; Dapprich, S.; Millam, J. M.; Daniels, A. D.; Kudin, K. N.; Strain, M. C.; Farkas, O.; Tomasi, J.; Barone, V.; Cossi, M.; Cammi, R.; Mennucci, B.; Pommelli, C.; Adamo, C.; Clifford, S.; Ochterski, J.; Petersson, G. A.; Ayala, P. Y.; Cui, Q.; Morokuma, K.; Malick, D. K.; Rabuck, A. D.; Raghavachari, K.; Foresman, J. B.; Cioslowski, J.; Ortiz, J. V.; Stefanov, B. B.; Liu, G.; Liashenko, A.; Piskorz, P.; Komaromi, I.; Gomperts, R.; Martin, R. L.; Fox, D. J.; Keith, T.; Al-Laham, M. A.; Peng, C. Y.; Nanayakkara, A.; Challacombe, M.; Gill, P. M. W.; Johnson, B. G.; Chen, W.; Wong, M. W.; Andres, J. L.; Gonzales, C.; Head-Gordon, M.; Repogle, E. S.; Pople, J. A. *Gaussian 98*, Rev. A7-A11; Gaussian, Inc.: Pittsburgh, PA, 1998.
(56) Johnson, B. G.; Gill, P. M. W.; Pople, J. A. *J. Chem. Phys.* **1993**, *98*, 5612.

dependent polarizability are calculated, whereby the former correspond to vertical excitation energies and the latter to oscillator strengths. We employed the density-functional-based implementation of this method (TD-DFT)[58] using again the B3LYP functional and the 6-31G* basis set described above.

The open-shell states of the singlet nitrenes[19] require at least two Slater determinants for a qualitatively correct description. We therefore resorted to the CASSCF/CASPT2 protocol[59] to calculate the energies of singlet nitrenes, the transition states for their different cyclization reactions, and the products of these cyclizations (cf. Figures 6 and 7). To "anchor" the DFT results on a common energy scale, we also recalculated the triplet phenylnitrenes at this multideterminantal level. All geometries were fully optimized by the CASSCF procedure, using an active space comprising 14 electrons in 12 molecular orbitals. In addition to 12 π-MOs (six on the phenyl ring, six on the pyrazolyl ring), the active space included two σ-MOs. In the nitrenes these were the singly occupied in-plane p-AO on the N atom and the in-plane lone pair on the same atom. In the cyclization transition states the former MO turned into the incipient C−N σ-bonding MO, whereas in the final products it was usually replaced by a higher lying σ(C−C) MO.

The above active spaces resulted in zero-order wave functions that consistently described the CASPT2 wave functions to over 66% in the parent compound and over 63% in the dimethyl compounds, thus ensuring that inclusion of dynamic electron correlation by many-body perturbation theory produces no artifacts. The [C,N]3s2p1d/[H]2s ANO basis set[60] was used in the CASSCF/CASPT2 calculations, which were carried out with the MOLCAS program.[61]

Full sets of Cartesian coordinates and absolute energies from all calculations (including thermal corrections in the case of B3LYP results) are given in the Supporting Information.

Acknowledgment. This work was supported by the Swiss National Science Foundation (project no. 200020-105217). We are very indebted to Krzysztof Piech for mapping the potential surfaces of the azides and the triplet nitrenes at the DFT level.

Supporting Information Available: Cartesian coordinates and energies (including enthalpies and free energies where available) of all stationary points discussed in this study (text file), relaxed potential energy surface scan of azide **1b**, and IR spectrum of didehydroazepine **15b** (pdf). This material is available free of charge via the Internet at http://pubs.acs.org.

JA043988W

(57) Casida, M. E. In *Recent Advances in Density Functional Methods;* Chong, D. P., Ed.; World Scientific: Singapore, 1995; Part I, p 155.
(58) Stratmann, R. E.; Scuseria, G. E.; Frisch, M. J. *J. Chem. Phys.* **1998**, *109*, 8218.
(59) Andersson, K.; Roos, B. O. In *Modern Electronic Structure Theory*; World Scientific Publ. Co.: Singapore, 1995; Part 1, Vol. 2, p 55.
(60) Pierloot, K.; Dumez, B.; Widmark, P.-O.; Roos, B. O. *Theor. Chim. Acta* **1995**, *90*, 87.
(61) Andersson, K.; Blomberg, M. R. A.; Fülscher, M. P.; Kellö, V.; Lindh, R.; Malmqvist, P.-Å.; Noga, J.; Olson, J.; Roos, B. O.; Sadlej, A.; Siegbahn, P. E. M.; Urban, M.; Widmark, P.-O. *MOLCAS*, versions 4 and 5; University of Lund: Lund, Sweden, 1998.